

60th Conference on Glass Problems
Sponsored by the Departments of Materials Science and Engineering at the
University of Illinois at Urbana-Champaign and Ohio State University
Urbana-Champaign, IL, October 18-20, 1999

RECEIVED
JUN 09 2000
OSTI

**MEASUREMENTS OF ALKALI CONCENTRATIONS IN AN OXYGEN-NATURAL
GAS-FIRED SODA-LIME-SILICA GLASS FURNACE**

Steven G. Buckley,* Peter M. Walsh,† David W. Hahn,§ and Robert J. Gallagher
Sandia National Laboratories, Livermore, CA

Mahendra K. Misra, John T. Brown, and Frederic Quan
Corning Incorporated, Corning, NY

Kanwal Bhatia and Vincent I. Henry
Visteon Automotive Systems, Dearborn, MI

R. Douglas Moore
Gallo Glass Company, Modesto, CA

The submitted manuscript has been authored by a contractor of the United States Government under contract. Accordingly the United States Government retains a non-exclusive, royalty-free license to publish or reproduce the published form of this contribution, or allow others to do so, for United States Government purposes.

Abstract

Sodium species vaporized from melting batch and molten glass in tank furnaces are the principal agents of corrosion of superstructure refractory and main contributors to emissions of particulate matter from glass melting. The use of oxygen in place of air for combustion of natural gas reduces particulate emissions, but is thought to accelerate corrosion in some melting tanks. Methods for measuring sodium are under investigation as means for identifying the volatilization, transport, and deposition mechanisms and developing strategies for control. Three separate methods were used to measure the concentrations of sodium species at various locations in an oxygen-natural gas-fired soda-lime-silica glass melting tank. Measurements were made inside the furnace using the absorption of visible light and in the flue duct using Laser-Induced Breakdown Spectroscopy (LIBS). Measurements in both the furnace and flue were also made by withdrawing and analyzing samples of the furnace gas.

*Present address: Dept. of Mechanical Engineering, University of Maryland, College Park, MD.

†Corresponding author: Sandia National Laboratories, Mail Stop 9051, Livermore, CA 94551.

§Present address: Dept. of Mechanical Engineering, University of Florida, Gainesville, FL.

DISCLAIMER

This report was prepared as an account of work sponsored by an agency of the United States Government. Neither the United States Government nor any agency thereof, nor any of their employees, make any warranty, express or implied, or assumes any legal liability or responsibility for the accuracy, completeness, or usefulness of any information, apparatus, product, or process disclosed, or represents that its use would not infringe privately owned rights. Reference herein to any specific commercial product, process, or service by trade name, trademark, manufacturer, or otherwise does not necessarily constitute or imply its endorsement, recommendation, or favoring by the United States Government or any agency thereof. The views and opinions of authors expressed herein do not necessarily state or reflect those of the United States Government or any agency thereof.

DISCLAIMER

Portions of this document may be illegible in electronic image products. Images are produced from the best available original document.

LIBS has been under development at Sandia and at other laboratories for some time as a technique for measuring part-per-billion levels of metals in particles suspended in gas streams. The LIBS instrument, mounted on a stack, focuses the light from a pulsed Nd:YAG laser in the gas/particle mixture to be analyzed. The spark caused by electric breakdown at the focal point produces an emission spectrum in which the wavelengths of the spectral lines are characteristic of the elements present and the intensities of the lines are related to their concentrations. The LIBS instrument demonstrated its capability as a real-time monitor during 10 hours of measurements of the total sodium concentration in high temperature particle-laden flue gas. The mole fractions of sodium were in the range 60 ± 10 mol ppm. Silicon and calcium were also observed, along with lithium, potassium, magnesium, and other minor and trace elements.

Concentrations of sodium atoms were also measured in the combustion space of the same melting tank using light absorption by the sodium D-lines. Total sodium species concentrations were derived from the atom concentrations assuming local chemical equilibrium. A typical total sodium mole fraction was 125 ppm, with higher and lower levels observed at the glass discharge and batch charge ends of the furnace, respectively. Using the measurement closest to the furnace exit, a value of 39 ± 15 mol ppm was expected at the sampling point in the flue, after accounting for dilution and the addition of sodium in the flue gas quench water. The levels of sodium measured near the furnace wall using the extractive sampling technique were lower, typically 30 mol ppm, with a high value (173 mol ppm) observed in one corner at the glass discharge end. In the flue, extractive sampling indicated a sodium mole fraction of 31 ± 16 ppm, in agreement with the estimate based on the absorption measurement in the furnace, but lower than the LIBS measurement at the same location in the flue.

The goal of the measurements is to identify routes of sodium transport and deposition, provide data for validation of numerical models for processes contributing to refractory corrosion and particulate emissions, and identify operating conditions under which sodium volatilization can be minimized.

Introduction

The development and application of oxy-fuel technology for glass melting furnaces was recently the subject of a workshop organized by the Glass Manufacturing Industry Council (Washington, DC, February 10, 1999), the topic of a session at the 18th International Congress on Glass (Choudhary, Huff, and Drummond, 1998), and the focus of an issue of the *GlassResearcher* (NY State College of Ceramics at Alfred University, 1998), including a useful bibliography of publications on oxygen-fuel firing (Longobardo, 1998). Oxygen-fuel firing has been a major theme of the Conferences on Glass Problems for a decade or more. The steady increase in number of container, fiber, and specialty glass melting tanks converted from air to oxygen-fuel firing is convincing evidence that the benefits from conversion outweigh the costs, at least in those sectors of the industry. The opening, in July 1998, of a rebuilt float glass tank at the Pilkington Libbey-Owens-Ford plant in Rossford, OH, marks the debut of oxygen-fuel firing in the last of the major industry sectors to adopt the technology.

The advantages of using oxygen: decreased capital cost, higher energy efficiency, reduced emissions of NO_x , SO_x , particulate matter, and CO_2 per unit mass of glass, increased throughput per unit area of melter, and more consistent product quality are well documented (Moore and Brown, 1991; Schroeder, 1998). An economic analysis by Benedek et al. (1996) concluded that requirements for two such benefits were sufficient to make oxygen competitive

with air firing, e.g. a need to comply with strict environmental regulations combined with a desire to increase production.

There are a number of technical questions associated with the design, construction, and operation of oxygen-natural gas-fired glass furnaces on which no industry-wide nor industry-sector-wide consensus has yet emerged. Among these are optimum tank dimensions, burner design and placement, choice of superstructure refractories, and means to control refractory corrosion. Most workers agree that, at this early stage in the evolution of oxygen-fired glass furnaces, many further opportunities for improvements in performance remain. The specific problem most often mentioned in connection with oxygen firing in soda-lime-silica glass furnaces is accelerated corrosion of superstructure refractories and its impact on furnace life.

The mechanism of corrosion of silica crown refractory by sodium and other alkali metal vapor species is discussed by LeBlanc (1996), Faber and Verheijen (1997), Godard et al. (1997), Kotacska and Cooper (1997), Misra et al. (1998), and Paskocimas et al. (1998). Two distinct processes are reported: (1) corrosion of the hot face exposed to combustion products and (2) formation of cavities in the refractory connected by narrow channels to the hot face ("rat holing"). There is agreement that the corrosive agents in both cases are derived primarily from vapor-phase sodium hydroxide, with possible contributions from other alkali metal species, but there is less agreement on the details of the reactions occurring at the silica surface. As emphasized by LeBlanc (1996), neither type of corrosion is universally observed in all oxygen-fired furnaces. A number of strategies for minimizing corrosion when it does occur have already emerged. Although reduction in the length of furnace campaigns after conversion from air to oxygen firing is often mentioned, it is the total quantity of glass pulled during campaigns before

and after conversion that is more useful as a basis for comparison. An even better basis would be the total yield of acceptable product during a campaign, but this is more difficult to document.

Most investigators agree that the condition having the greatest influence on the rate of crown refractory corrosion is the local concentration of vapor phase sodium species in the combustion products adjacent to the refractory surface. Temperature, gas velocity, and gas composition are also important, but thought to have less influence than sodium concentration. The most abundant sodium-containing vapor species under most conditions relevant to melting tanks, either air or oxygen-fired, is NaOH, but free sodium atoms can be a significant fraction of the total sodium in the gas phase under some conditions. From the point of view of transport of sodium from the melt to the crown, it makes little difference which of the two, Na or NaOH, is most reactive toward silica. If either one of the species were removed preferentially by reaction with the surface, it would be quickly regenerated by reactions such as $\text{Na} + \text{H}_2\text{O} \rightarrow \text{NaOH} + \text{H}$ and $\text{NaOH} + \text{M} \rightarrow \text{Na} + \text{OH} + \text{M}$, where M is any of the molecules present, in conjunction with other elementary reactions which together would strive to maintain local chemical equilibrium in the gas phase.

The reported experience suggests that corrosion by alkali metal species is amenable to control. In developing a reliable strategy for control, three different, but complementary, approaches will be useful: (1) monitoring of sodium in the furnace exhaust to determine the overall conditions having the greatest influence on the cumulative sodium vaporization, (2) measurements of sodium species in the combustion space to identify the routes of sodium transport and deposition, and (3) numerical modeling of the entire process of vaporization, entrainment, transport, and deposition. The present paper describes a laser-based technique for monitoring sodium and other metals in furnace exhaust, a light absorption measurement of the

average concentrations of sodium along straight paths through the furnace, and an extractive method for sampling sodium as gas or as particles in either the furnace or the exhaust. The measurements are intended not only to address questions regarding local and cumulative sodium concentrations in the combustion space, but to provide data for testing and validation of numerical models for sodium species behavior. In the remainder of the paper, we first describe the site where the measurements were made, then devote one section to each of the measurement techniques, and finally compare and discuss the measurements themselves.

The Glass Furnace

The measurements were made in the combustion space and flue of Tank No. 1 in the Gallo Glass Company container plant in Modesto, CA. Tank No. 1 is the melter that was converted from air to oxygen firing in 1991, paving the way for the introduction of oxygen-natural gas technology into large glass furnaces (Moore and Brown, 1991). The measurements reported here were made following a recent rebuild. Conditions during the measurements were pull rate, 381 to 384 ton/day; natural gas flowrate, 46,000 scfh; oxygen to gas ratio 2.01 by volume; and electric boost 2.2 MW. The tank was melting flint container glass from batch containing 41.4 wt% cullet.

At Gallo Glass there are four oxygen-natural gas-fired melting tanks whose flues are all connected to a common duct. Because Tank No. 1 is at the upstream end of the system, its exhaust has not been mixed with that from any other furnace, so measurements of gas and particle composition in the flue are determined solely by conditions in Tank No. 1. The measurements in the flue have no relation to stack emissions, because particles are removed from the flue gas in an electrostatic precipitator serving all four of the oxygen-natural gas-fired melting tanks.

Measurements in the Flue Using Laser-Induced Breakdown Spectroscopy (LIBS)

Introduction to LIBS

Laser-induced breakdown spectroscopy (LIBS) has been used as an analytical technique for gases, liquids, and solids for some time (Schechter, 1997; Song et al., 1997). Applications of LIBS typically employ a pulsed laser with a high peak power to form a spark (breakdown) in the medium to be examined. In gases, the temperature of the resulting plasma is in the range of 10,000 – 15,000 K, hot enough to fragment all molecules into their constituent atoms, and to excite the electrons in the atoms out of the ground state and into excited electronic states. As the plasma cools, excited electrons relax back into their ground states, emitting light at characteristic atomic frequencies. Identification of the atoms present in the sample volume occurs using well-known atomic emission lines, and quantification of the atomic species concentration occurs via quantification of the intensity of the atomic emission lines. Sensitivities range from parts-per-billion (ppb) for some species, such as Be, to well above the parts-per-million (ppm) level for other species, such as Sb.

A LIBS monitor was placed in the exhaust duct downstream from Tank No. 1. The goal of the LIBS portion of the work was to make real-time, in situ measurements of sodium in the duct. In addition, snapshot measurements of other species (e.g. Ca, Mg, K) were made to obtain a semi-quantitative determination of their concentration. Conditions in the duct were relatively severe: 350 °F and 35 ft/sec flow velocity. When the flue gas reaches the sampling point, the sodium that was present in the combustion space as atomic sodium and sodium hydroxide vapors has reacted with sulfur dioxide, oxygen, and additional species. This has further nucleated, condensed, and coagulated in the cooling flue gas to form small submicrometer particles. Some condensation on preexisting particles such as those entrained from the batch blanket is also

expected. Under the conditions of temperature and gas composition in the flue, the predominant sodium species is typically solid sodium sulfate. As will be discussed, the flow velocity presented a considerable challenge to making the measurements.

LIBS Experimental Methods

The Sandia LIBS-based metals CEM utilizes a 1064-nm Nd:YAG laser as the excitation source, with a nominal pulse width of 10 ns and pulse energy of 400 mJ. The laser beam is expanded to 12 mm and then focused to create the plasma using a 75-mm focal length, 50-mm diameter UV-grade quartz lens. The 50-mm lens also functions to collect the plasma and atomic emission. A schematic of the LIBS monitor system is presented in Figure 1. LIBS spectra are nominally collected at 5 Hz using an Acton 0.25-m spectrometer and Princeton Instruments time-gated CCD array. Communications delays make the true acquisition rate approximately 3 Hz. The CCD intensifier gate width used for the most of the species measured at the Gallo field test was 150 μ s, with a time delay of 50 μ s from the laser pulse. A delay and gate of 10 μ s and 4 μ s, respectively, were used for Na measurements. The complete system is controlled remotely by a PC-based computer. The laser system was mounted on a roof where good access to the exhaust duct in which the measurements were to be made was available, while the remote computer (connected via fiberoptic cable) was located in an air conditioned rental truck approximately 100 feet away.

The output spectrum contains a continuous background emission signal with superimposed discrete atomic emission line signals. A typical LIBS spectrum is shown in Figure 2. This spectrum is a 500-shot average showing two peaks from Ca^+ (393.4 and 396.8 nm), two peaks from K (404.4 nm and 404.7 nm, incompletely resolved), and a peak from Pb (405.8 nm). For each targeted analyte emission line, a LIBS signal is calculated based on the integrated

emission line peak divided by the surrounding continuous background intensity level. A concentration is calculated from a library of linear calibration curves entered for each target analyte atomic emission line, as determined in the laboratory using a calibration flow stream of known mass concentration, and with identical LIBS parameters (e.g. lens focal length, laser power) as utilized for the field measurements. Figure 3 illustrates the calibration used for the 589.5 nm sodium emission line.

Previous work has shown that a linear calibration works quite well for relatively low concentrations, i.e. in the range 10 ppb – 10 ppm. For this study, the maximum concentration that we were able to flow through our calibration system was 11 ppm, due to plugging of the atomizer orifice at higher concentrations. Due to this fact, we were unable to calibrate the instrument at concentrations as high as those measured in the glass furnace for Na and K, and had to extrapolate the linear calibration curve to concentrations as high as 60 ppm. At these higher concentrations we expect that there is a possibility of limited self-absorption, which would cause the reported concentration to be somewhat lower than the true concentration. No attempt was made to correct for this possibility in the data.

LIBS Results

The high flow velocity and the substantial concentration of hot, sticky, alkali-containing particles hampered initial measurements in the exhaust of the glass furnace. The LIBS instrument that we used for these measurements was designed for incinerator exhaust environments, where both the flow velocity and the particle loading are much lower than encountered in the glass furnace exhaust duct. Figure 4 illustrates difficulties encountered during the initial measurements. For a given laser pulse energy, the baseline signal reflects a measure of light transmission to and from the focal volume (or an inverse measurement of the absorption of

the light). As shown in the figure, the value of the baseline signal fell substantially during a given 90-minute period. In contrast, the measured corrected signal (peak/baseline) rose substantially during this period. These results were due to the fact that the lens was becoming coated with tiny sodium-containing particles. These particles absorbed the light travelling to and from the lens focus where the breakdown should occur, resulting in a reduced background signal with time. In addition, the sodium in the particles coating the lens could have been excited by the laser, resulting in sodium emission and a corrected signal that increased with time. Increasing the nitrogen purge flow rate for the lens did not solve the problem.

The solution for the lens coating problem was to fashion a cylindrical metal shroud for the lens, with a hole in the end just large enough for the laser beam. The shroud was pressurized with a positive pressure of nitrogen, so that gas flowed out of the shroud with a substantial velocity. Increasing and decreasing the flow velocity under constant conditions yielded consistent concentration measurements, proving that the nitrogen flow was not interfering with the sodium concentration in the measurement volume (10 cm from the lens).

Using this configuration, we were able to obtain consistent results, and no evidence of lens coating was observed. Figures 5a and 5b illustrate Na time series data from August 18 and August 19, 1998, respectively, reported in 72-second increments. Each data point represents the average of 200 shots. On August 18, Na concentrations between 53 and 67 mole-ppm were observed, with a mean concentration of 59.5 ppm and a standard deviation of 3.2 ppm. On August 19, Na concentrations between 49 and 69 mole-ppm were observed, with a mean concentration of 58.3 ppm and a standard deviation of 4.7 ppm. No rapid fluctuations in Na concentration are noted, but trends with time (± 5 ppm over the period of 30 minutes) may be observed on both days. For example, the first three hours of data from August 19 exhibit a mean

concentration of 55 mol ppm, while the second three hours exhibit an average concentration of 62.5 mol ppm. As might be expected from the large thermal mass of the furnace, changes in the Na emission rate appear to occur slowly, over long time scales.

A number of other elements were also observed at lower concentrations than the sodium. Calibrations for the elements whose emission lines appear in Figure 2 suggest that the approximate concentrations of calcium and lead were 20 ppb and 1.1 ppm, respectively, while the potassium concentration was much higher than we could generate in our laboratory. A linear fit to low concentration calibration data using the 766.5 nm line would indicate that the potassium concentration was greater than 40 ppm. Similar spectra indicate approximate concentrations of 60 ppb for Cr, 100 ppb for Mg, and 1.3 ppm for Si. In addition, B, Cd, Li, and Zr were also observed. It is emphasized that the reported concentrations for these elements are approximate, based only on 500-shot (3-minute) averages.

Measurements in the Combustion Space Using Light Emission/Absorption

Introduction to the Emission/Absorption Measurements

The D-lines of sodium at 589.0 and 589.6 nm, in the yellow region of the visible spectrum, are the most prominent features in the spectrum of near-UV, visible, and near-IR radiation emitted from the combustion space of air-natural gas and oxygen-natural gas-fired soda-lime-silica glass melting tanks. The intensities of light absorbed and emitted near these wavelengths can be used to measure the gas temperature and sodium concentration in the combustion space. Optical techniques are attractive because the environment inside a furnace is so hostile and because it is desirable to minimize disturbance to the gas while making measurements. Gas temperatures, particularly at some locations in oxygen-gas-fired furnaces, are too high to measure using traditional methods, such as a platinum-rhodium thermocouple in a

suction pyrometer. There is a substantial literature on the application of emission-absorption pyrometry and spectrometry using the D-lines of sodium and potassium. Recent work may be found in papers by Thomas (1968), Daily and Kruger (1977), Onda et al. (1981), Paul and Self (1989), and Bauman (1994).

Principle of the Emission/Absorption Measurements

To make the measurements, a tungsten ribbon lamp having a higher brightness temperature than the gas is placed on one side of the furnace, and the spectrum of the light transmitted across the combustion space is observed on the opposite side using a spectrometer, as shown in Figure 6a. A second measurement, with the lamp turned off, gives the contribution to the observed intensity from emission of light by the hot gas in the combustion space. The equation of radiative transfer through the emitting and absorbing medium, assumed to be at uniform temperature, is (the definitions of the symbols may be found in the Nomenclature Section):

$$I_{\lambda} = I_{\lambda,B}(T_{lamp}) \exp(-\kappa_{\lambda} n_{Na} l) + I_{\lambda,B}(T_{gas}) [1 - \exp(-\kappa_{\lambda} n_{Na} l)] \quad (1)$$

I_{λ} is the observed intensity at a given wavelength, $I_{\lambda,B}(T_{lamp})$ is the intensity of light from the calibrated lamp at the same wavelength, and $I_{\lambda,B}(T_{gas})$ is the intensity of thermal black body radiation at that wavelength at the temperature of the gas. The first term in Equation 1 is the contribution from the lamp and the second term is the contribution from the gas. Substitution of Wein's law, describing the relationship between temperature and the intensity of black body radiation, provides a relationship between the measured intensities and the temperature of the gas:

$$T_{gas} = \frac{1}{\frac{1}{T_{lamp}} + \frac{\lambda k}{hc} \ln \left[\frac{I_{\lambda,gas} + I_{\lambda,lamp} - I_{\lambda,gas+lamp}}{I_{\lambda,gas}} \right]} \quad (2)$$

The concentration of sodium atoms is found from

$$\frac{I_{\lambda, gas+lamp} - I_{\lambda, gas}}{I_{\lambda, lamp}} = \exp(-\kappa_{\lambda} n_{Na} l) \quad (3)$$

which is Beer's law, with the contribution of emission from the gas, the second term in the numerator on the left-hand side, subtracted from the measured gas-plus-lamp signal. Because the intensities in Equations 2 and 3 appear as ratios, no absolute measurement of intensity is ever required, provided that the geometry of the optical system is not changed while recording the emission and absorption spectra.

Interpretation of the Emission/Absorption Measurements

Two problems arise in the interpretation of the absorption measurements to determine concentrations of sodium. The first is that the measurement provides the concentration only of free sodium atoms, but the property of greatest interest is the concentration of all sodium-containing species, because all contribute to refractory corrosion and the formation of particulate matter. This problem was resolved by using the NASA Lewis Chemical Equilibrium Code (McBride and Gordon, 1996) to calculate the distribution of sodium-containing species at equilibrium as a function of temperature. The ratio of sodium atoms to total sodium was fit by an Arrhenius-type function used to estimate total sodium from the measurements of sodium atoms and gas temperature. Atomic sodium and sodium hydroxide were the major sodium-containing species under all conditions.

The other problem which arose in the calculation of sodium concentrations was finding published values for the absorption coefficient in the region of the spectrum where conditions dictated that the measurements be made. Because sodium is a strong absorber, because its concentration in the combustion space is substantial (10 - 200 mol ppm), and because the path length through the furnace is long, the gas behaves as a black body over a broad range of

wavelengths at the center of the D-lines. This can be seen by examining the behavior of Equation 1 for large values of the exponent, $\kappa_{\lambda} n_{Na} l$, when $I_{\lambda} \cong I_{\lambda, B}(T_{gas})$. Neither Equation 2 nor Equation 3 is applicable under these conditions. The region where the equations do apply is very far from line center, in a range of wavelengths where very little data on the shape of the D-lines is available. One study, by Jongerius and coworkers (1981a, 1981b), does provide sufficient information to permit estimation of the absorption coefficients for sodium atoms over the range of wavelengths needed. Line shapes for sodium atoms were given by these workers in mixtures of nitrogen and water vapor at 500 and 2000 K. The line broadening data for nitrogen were used in place of those for carbon dioxide to estimate the line shape in the products of oxygen-natural gas combustion at 2000 K. Because the temperature dependence is not known, the data for 2000 K were used in all cases. Fortunately, the effect of temperature is very weak, except for its effect on the total gas molecule number concentration which was included in the calculations, and 2000 K is close to the actual temperatures in the combustion space.

Results of the Emission/Absorption Measurements

Using the sodium D-line emission and absorption measurements, calculations of temperature and sodium concentration were performed at a number of wavelengths across the D-lines to check for systematic errors. The temperatures calculated at all wavelengths agreed quite well. The sodium concentrations, however, differed from one side of line center to the other, a discrepancy which probably arises from the approximations introduced in determining the wavelength dependence of the absorption coefficient, as described above.

The average gas temperature and total sodium species mole fraction (primarily Na and NaOH) were determined through every available pair of peepholes along the length of the Gallo Glass Co. furnace, as shown in Figure 6. Three sets of measurements were taken, in December

1997, August 1998, and in September/October 1998. Some differences in the axial profiles were observed, especially at the batch feed and glass discharge ends of the furnace. The differences may arise from differences in air infiltration with change in furnace pressure and condition of the furnace. The profile of gas temperatures along the length of the furnace during the August 1998 measurement campaign is shown in Figure 6b. Gas temperatures in the middle of the furnace were in the range from 2000 to 2100 K (1700 to 1800 °C, 3100 to 3300 °F). Lower gas temperatures were observed at the ends, especially over the batch blanket, where the average temperature was 1650 K (1375 °C, 2500 °F).

The profile of total sodium species mole fractions along the length of the furnace is shown in Figure 6c. A typical sodium level near the middle of the furnace was 125 mol ppm. Sodium increased almost by a factor of 2 in the relatively stagnant gas toward the glass discharge end, and decreased markedly over the batch blanket. The latter observation does not necessarily imply that the melting batch is not a significant source of sodium because the gas along the line of sight from peephole to peephole may have been diluted by air entering through the batch feeder. A separate set of measurements, at higher excess oxygen, showed neither the high sodium level at the discharge end nor the low sodium level at the charge end of the furnace, the mole fraction being roughly the same at all of the observation points.

We are presently working on the extraction of information about the transverse temperature profile across the furnace using the width and depth of the self absorption feature that appears in the D-line spectrum close to line center, where light emitted by hot gas at the center of the furnace is absorbed by cooler gas in the boundary layer at the furnace wall.

Measurements in the Combustion Space and Flue by Extractive Sampling

A method for determination of sodium and other metals, present either as vapor or as suspended particles, by extractive sampling of combustion products from furnaces and ducts, was developed by Tong, Brown, and Kotacska (1997). The gas and particles are withdrawn through a platinum tube and the metals are separated by bubbling the gas through water-filled impingers. The probe and transfer lines are washed to recover material deposited there during sampling and the impinger water and wash water are analyzed in the laboratory for the species of interest. In the case of sodium, the analysis is done using a specific ion electrode. The extractive technique is especially attractive because of its simplicity and will always be a useful method for checking other techniques. One can even envision an extractive system that would provide real time measurements, for example by measuring the metal concentration in condensate extracted through a water-cooled probe, using a specific ion electrode or other rapid analytical technique.

The results of extractive sampling in the combustion space and flue are shown in Figure 7. The typical sodium level in the furnace, in the region probed using the platinum tube, close to the furnace wall, was 30 mol ppm. One high value, 173 mol ppm, was observed in a corner close to the glass discharge end. Three separate determinations of the sodium content of the flue gas were 22.7, 19.6, and 49.3 mol ppm, giving an average of 31 mol ppm and a standard deviation of 16 mol ppm.

Comparison and Discussion of the Results

There is encouraging correspondence between the sodium measurements by light absorption and extractive sampling in the furnace. The extractive measurement at the wall over the batch blanket (23 mol ppm, Figure 7) is in good agreement with the absorption measurement across the top of the blanket (18.5 ± 6.3 mol ppm, Figure 6c). One of the extractive

measurements at the glass discharge end (173 mole ppm, Figure 7) is also in good agreement with the absorption measurement across that end of the furnace (228 ± 65 mol ppm, Figure 6c). The measurements by extractive sampling near the wall in the middle of the furnace are lower than the absorption measurements by approximately a factor of four. This may be due to dilution of the combustion products by in-leaking air near the wall where the extractive sampling was done. On the other hand, a number of assumptions were made in the estimation of the total sodium species mole fractions from the light absorption data, such as that the gas temperature and sodium mole fractions were uniform along the light path, and that the sodium vapor species were in equilibrium. The effects of these approximations are under examination and will be reported as the work progresses.

By analyzing the flue gas for oxygen, combustion products formed at burner oxygen/natural gas ratio were estimated to have been diluted by a factor of 3.8 on arrival at the sampling point in the flue, including the effects of air infiltration and water injected into the flue gas to lower its temperature. Samples of the city water were analyzed for sodium. From the average sodium content of those samples and the measured water flow rate, the water was estimated to contribute 4 mol ppm of sodium to the flue gas. The total sodium in the gas approaching the furnace exit was 134 ± 57 mol ppm (point at the distance of 5.5 m from the batch blanket charger in Figure 6c). Assuming that this is the mole fraction in undiluted combustion products, the mole fraction of sodium at the sampling point in the flue is expected to be 39 ± 15 mol ppm, in good agreement with the direct measurement of sodium in the flue, 31 ± 16 mol ppm, using the extractive sampling technique. These values are lower than the measurements of total sodium in the flue using LIBS: 59.5 ± 3.2 mol ppm on August 18 (Figure 5a) and 58.3 ± 4.7 mol ppm on August 19 (Figure 5b). However, considering the approximations and assumptions

underlying each of the measurements and the difficult conditions under which the measurements were made, the consistency of the three independent sets of data is very encouraging.

One of the objectives of the work is to use the continuous, real-time measurements by LIBS to identify conditions under which the vaporization of sodium can be minimized. The data shown in Figures 5a and 5b do in fact show some significant long-term drifts in the sodium content of the flue gas. However, none of the flowrate or temperature records from the control room showed any obvious correlation with the sodium measurements. Evidently, a cross correlation of control room and sodium records will be needed to determine the conditions through which some degree of control over sodium volatilization can be achieved.

The objective of the measurements in the furnace is to provide insight into the mechanism of vaporization, transport, and deposition of sodium-containing species in the combustion space. The line of sight measurements are a first step in that direction, providing data with which the predictions of numerical simulations can be compared and tested.

Summary and Conclusions

Three different techniques were used to measure the mole fractions of sodium-containing species vaporized from soda-lime-silica glass in an oxygen-natural gas-fired melting tank: (1) extractive sampling of the gas and vapor near the wall in the combustion space, (2) absorption of light across the width of the furnace by the atomic sodium D-lines, and (3) emission of light after dissociation and excitation of sodium atoms in a plasma produced by focussing a pulsed Nd:YAG laser in the flue duct. The extractive technique indicated 15 to 43 mol ppm of sodium near the wall in the middle of the furnace, with a higher value (173 mol ppm) observed in one corner at the glass discharge end of the furnace and a low value (23 mol ppm) in one corner at the batch charge end. The absorption measurements were consistent with these qualitative

features, but indicated sodium concentrations integrated over the width of the furnace approximately four times higher than the concentrations near the wall. A possible explanation for this difference is dilution of the gas near the wall by inleaking air.

The results of measurements in the flue were: by extractive sampling, 31 ± 16 mol ppm; and using LIBS, 59.5 ± 3.2 and 58.3 ± 4.7 mol ppm on different days. The light absorption measurements in the furnace, after correction for dilution of the combustion products by air and steam, were expected to give 39 ± 15 mol ppm in the flue. LIBS demonstrated its ability to monitor sodium in the flue continuously and in real-time. Measurements over an extended period and cross correlation with gas and oxygen flowrates and glass and refractory temperatures are recommended to identify conditions that would minimize volatilization of sodium and its attack on superstructure refractories.

Acknowledgments

This work was supported by Corning Incorporated, Visteon Automotive Systems, and the U.S. Department of Energy, Office of Industrial Technologies. The Project Managers were John T. Brown and Mahendra K. Misra (Corning), Vincent I. Henry and Kanwal Bhatia (Visteon), and Theodore R. Johnson (DOE/OIT Glass Vision Team). The authors thank the Gallo Glass Company for permission to make the measurements, Howard A. Johnsen and James R. Ross (both of Sandia), for their work on the set up of the LIBS instrument and collection of the LIBS data, Edward J. Walsh (Sandia) for his work on the LIBS data acquisition software, and Phillip H. Paul (Sandia) for many helpful discussions of the emission/absorption measurements.

Nomenclature

c	Speed of light, m s^{-1}
I_λ	Intensity of radiation at wavelength, λ , $\text{W steradian}^{-1} \text{m}^{-1}$
$I_{\lambda, \text{gas}}$	Intensity of radiation at wavelength, λ , from the gas alone, with the lamp off, $\text{W steradian}^{-1} \text{m}^{-1}$
$I_{\lambda, \text{lamp}}$	Intensity of light from the lamp at wavelength, λ , if the gas were neither emitting nor absorbing, $\text{W steradian}^{-1} \text{m}^{-1}$
$I_{\lambda, \text{gas+lamp}}$	Intensity of light at wavelength, λ , when the gas is illuminated by the lamp, including the radiation emitted by the gas, $\text{W steradian}^{-1} \text{m}^{-1}$
$I_{\lambda, B(T_{\text{gas}})}$	Intensity of radiation emitted from a black body at wavelength, λ , $\text{W steradian}^{-1} \text{m}^{-1}$
$I_{\lambda, B(T_{\text{lamp}})}$	Intensity of radiation emitted at wavelength, λ , from a black body at the brightness temperature of the lamp, $\text{W steradian}^{-1} \text{m}^{-1}$
h	Planck constant, J s
k	Boltzmann constant, J K^{-1}
l	Width of the furnace, breastwall to breastwall, m
n_{Na}	Number concentration of sodium atoms, m^{-3}
T_{gas}	Gas temperature, K
T_{lamp}	Brightness temperature of the lamp, K
κ_λ	Absorption coefficient of sodium atoms at wavelength, λ , m^{-2}
λ	Wavelength, m

References

- Bauman, L. E., "Investigation of MHD Flow Structure and Fluctuations by Potassium Lineshape Fitting," *Combustion and Flame* 98 (1994) 46-58.
- Benedek, K., M. Morgan, R. Wilson, V. Hobbs-Moore, and L. Donaldson, "Industry Drivers and Economics of Oxy-Gas Use in the U.S. Glass Industry," American Flame Research Committee, Spring Members' Technical Meeting, Orlando, FL, May 6-7, 1996.
- Choudhary, M. K., N. T. Huff, and C. H. Drummond (Eds.), *Proceedings of the XVIII International Congress on Glass*, American Ceramic Society, Westerville, OH, 1998.
- Daily, J. W. and C. H. Kruger, "Effects of Cold Boundary Layers on Spectroscopic Temperature Measurements in Combustion Gas Flows," *Journal of Quantitative Spectroscopy and Radiative Transfer* 17 (1977) 327-338.
- Faber, A. J. and O. S. Verheijen, "Refractory Corrosion under Oxy-Fuel Firing Conditions," *Ceramic Engineering and Science Proceedings* 18, Issue 1 (1997) 109-119.
- Glass Manufacturing Industry Council, *Oxy-Fuel Issues II: Approaching the New Millennium*, Washington, DC, February 10, 1999.
- Godard, H. T., L. H. Kotacska, J. F. Wosinski, S. M. Winder, A. Gupta, K. R. Selkregg, and S. Gould, "Refractory Corrosion Behavior under Air-Fuel and Oxy-Fuel Environments," *Ceramic Engineering and Science Proceedings* 18, Issue 1 (1997) 180-207.
- Jongerius, M. J., A. R. D. Van Bergen, Tj. Hollander, and C. Th. J. Alkemade, "An Experimental Study of the Collisional Broadening of the Na-D Lines by Ar, N₂, and H₂

Perturbers in Flames and Vapor Cells - I. The Line Core," *Journal of Quantitative Spectroscopy and Radiative Transfer* 25 (1981a) 1-18.

Jongorius, M. J., Tj. Hollander, and C. Th. J. Alkemade, "An Experimental Study of the Collisional Broadening of the Na-D Lines by Ar and N₂ Perturbers in Flames and Vapor Cells - II. The Line Wings," *Journal of Quantitative Spectroscopy and Radiative Transfer* 26 (1981b) 285-302.

Kotacska, L. H. and T. J. Cooper, "Testing of Superstructure Refractories in a Gas-Oxy Atmosphere Against High-Alkali Glasses," *Ceramic Engineering and Science Proceedings* 18, Issue 1 (1997) 136-145.

LeBlanc, J., "Controlling Silica Attack on Soda Lime Oxy-Fuel Furnaces," *Ceramic Industry* 146, June 1996, pp. 27-29. "Impact of Silica Attack on Soda Lime Oxy-Fuel Furnaces," *Glass Technology* 37, No. 5 (1996) 153-155.

Longobardo, A., "Bibliography: Oxy-Fuel Technology for Glassmaking," *The GlassResearcher*, Vol. 8, No. 1, Summer 1998. New York State College of Ceramics at Alfred University, Alfred, NY.

McBride, B. J. and S. Gordon, "Computer Program for Calculation of Complex Chemical Equilibrium Compositions and Applications, II. Users Manual and Program Description," NASA Reference Publication 1311, National Aeronautics and Space Administration, Lewis Research Center, Cleveland, OH, June 1996.

Misra, M. K., S. S. C. Tong, and J. T. Brown, "Superstructure Corrosion in Glass Tanks: Comparison of Mathematical Model with Field Measurements," *Ceramic Engineering and Science Proceedings* 19, Issue 1 (1998) 137-143.

Moore, R. D. and J. T. Brown, "Conversion of a Large Container Furnace from Regenerative Firing to Direct Oxy-Fuel Combustion," *Ceramic Engineering & Science Proceedings*, Vol. 13, Issue 3-4, 1992, pp. 18-24.

New York State College of Ceramics at Alfred University, Alfred, NY, *the GlassResearcher: Bulletin of Glass Science and Engineering*, Vol. 8, No. 1, Summer 1998.

Onda, K., Y. Kaga, and K. Kato, "Measurement of MHD Combustion-Gas Temperatures and Potassium Number Densities in the Presence of Cold Boundary Layers," *Journal of Quantitative Spectroscopy and Radiative Transfer* 26 (1981) 147-156.

Paskocimas, C. A., E. R. Leite, E. Longo, W. Kobayashi, M. Zorrozua, and J. A. Varela, "Determination of Corrosion Factors in Glass Furnaces," *Ceramic Engineering and Science Proceedings* 19, Issue 1 (1998) 75-88.

Paul, P. H. and S. A. Self, "Method for Spectroradiometric Temperature Measurements in Two Phase Flows. 1: Theory," *Applied Optics* 28 (1989) 2143-2149.

Schechter, I., "Laser Induced Plasma Spectroscopy: A Review of Recent Advances," *Reviews in Analytical Chemistry* 16 (1997) 173-298.

Schroeder, R. W., "Development of Oxy-Fuel Technology in the Glass Industry," *the GlassResearcher: Bulletin of Glass Science and Engineering*, Vol. 8, No. 1, Summer 1998, pp. 1, 3-4. New York State College of Ceramics at Alfred University, Alfred, NY.

Song, K., Y.-I. Lee, and J. Sneddon, "Applications of Laser-Induced Breakdown Spectrometry," *Applied Spectroscopy Reviews* 32 (1997) 183-235.

Thomas, D. L., "Problems in Applying the Line Reversal Method of Temperature Measurement to Flames," *Combustion and Flame* 12 (1968) 541-549.

Tong, S. S. C., J. T. Brown, and L. Kotacska, "Determination of Trace Impurities in a Furnace Atmosphere at Operating Temperature," *Ceramic Engineering & Science Proceedings*, Vol. 18, Issue 1, 1997, pp. 208-215.

Figure Captions

Figure 1. Laser-Induced Breakdown Spectroscopy (LIBS) monitor schematic.

Figure 2. Typical LIBS emission spectrum, showing the presence of calcium, potassium, and lead.

Figure 3. Linear calibration for the sodium emission line at 589.6 nm.

Figure 4. Sodium data without sufficient purge on the focusing lens.

Figure 5. Time-series data for sodium, measured using LIBS in the flue of Tank No. 1 at the Gallo Glass Company. a. August 18, 1998. b. August 19, 1998.

Figure 6. a. Plan of the furnace showing the locations of the burners and exhaust ports and the arrangement of the tungsten ribbon lamp and spectrometer for the emission/absorption measurements in the combustion space. b. Apparent gas temperatures along the line of sight across the width of the furnace. c. Total sodium species mole fractions averaged over the width of the furnace. Gallo Glass Company, Tank No. 1, August 24 - 28, 1998.

Figure 7. Total sodium species mole fractions near the furnace wall in the combustion space and in the flue, determined by extractive sampling and analysis using the method of Tong, Brown, and Kotacska (1997). Also shown are the mass flowrates of sodium in the two vertical flues, in the flue gas quench water, and in the horizontal flue duct where the LIBS measurements were made. Gallo Glass Company, Tank No. 1, August 18, 1998.

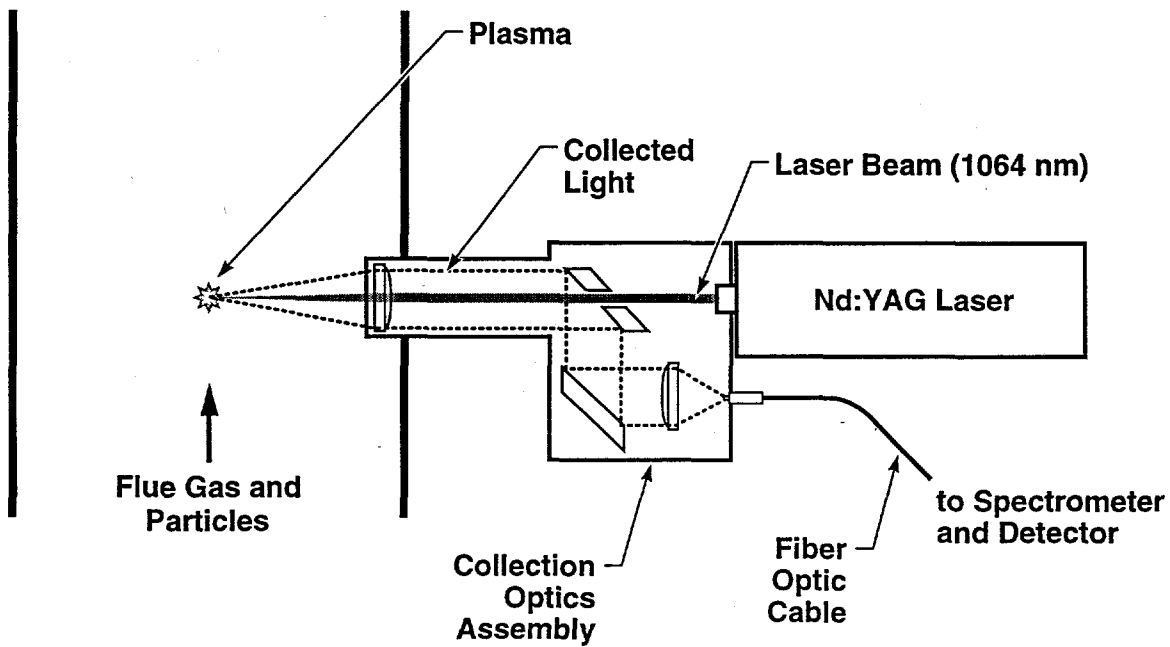


Fig. 1

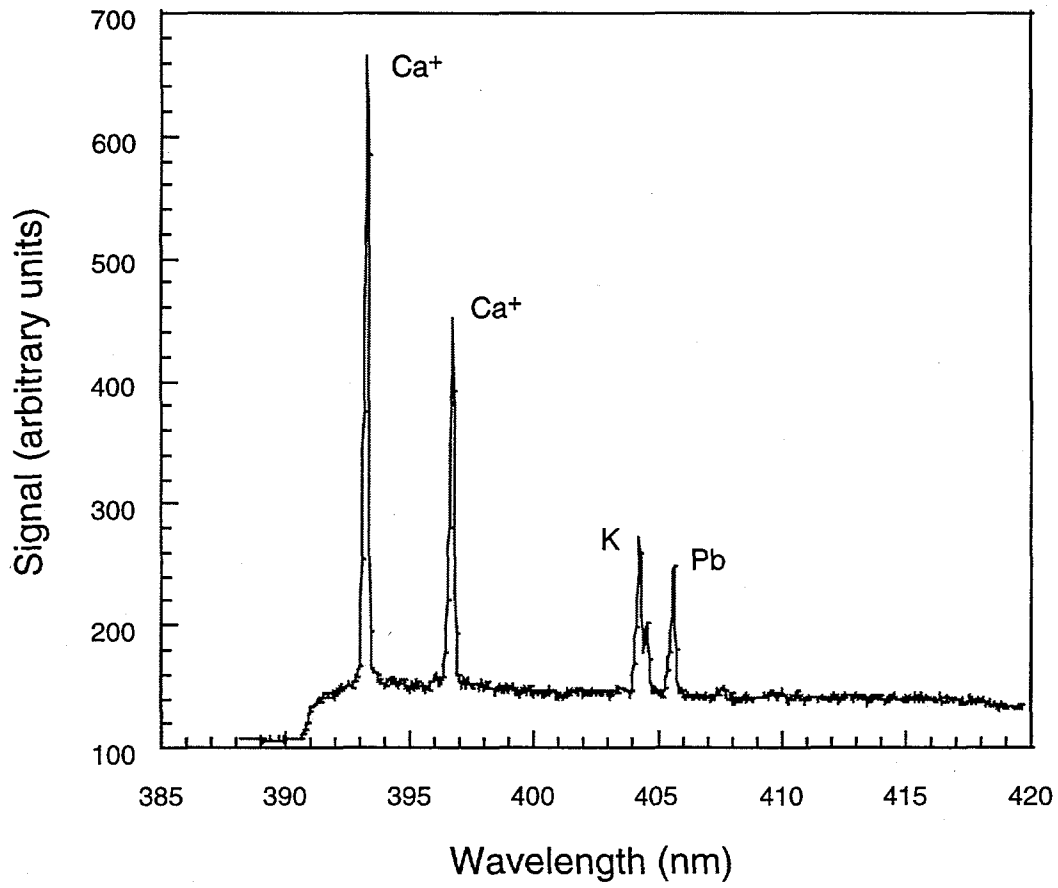


Fig. 2

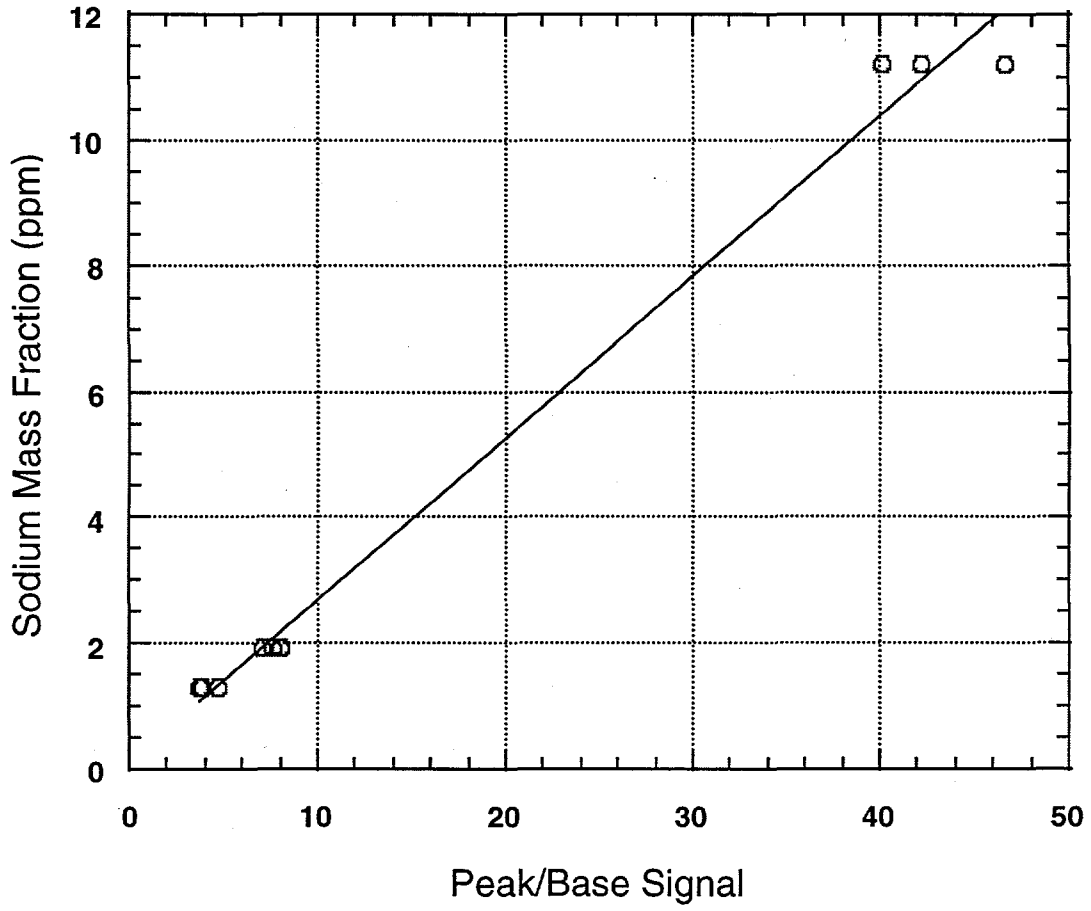


Fig. 3

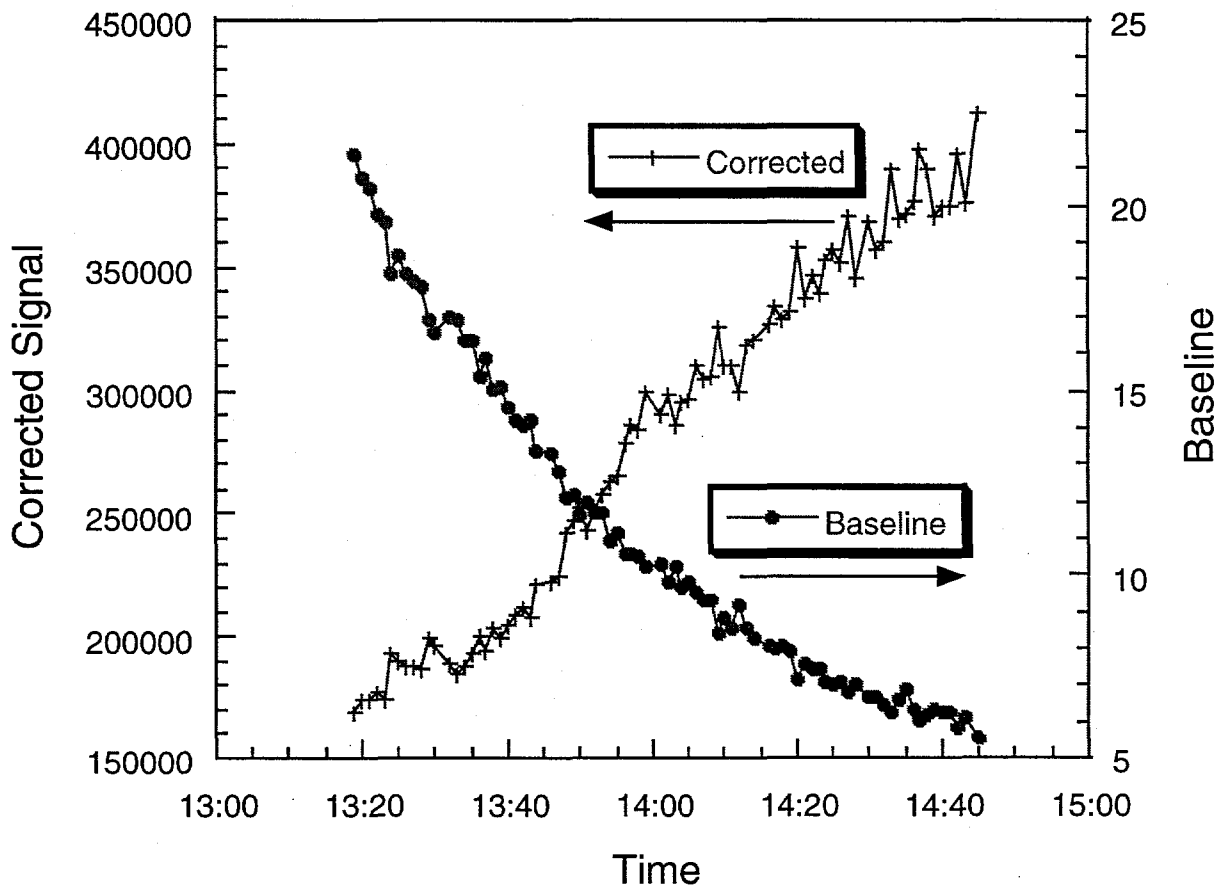


Fig. 4

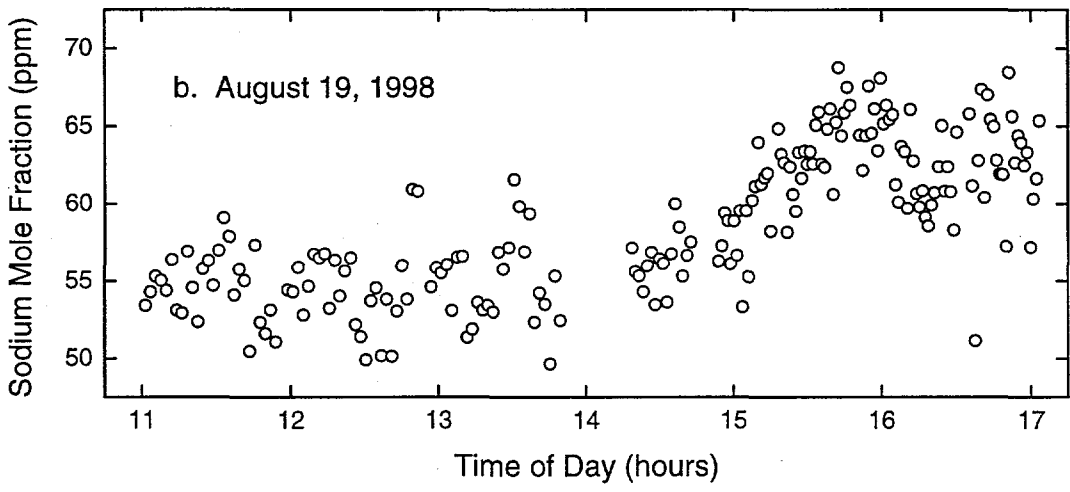
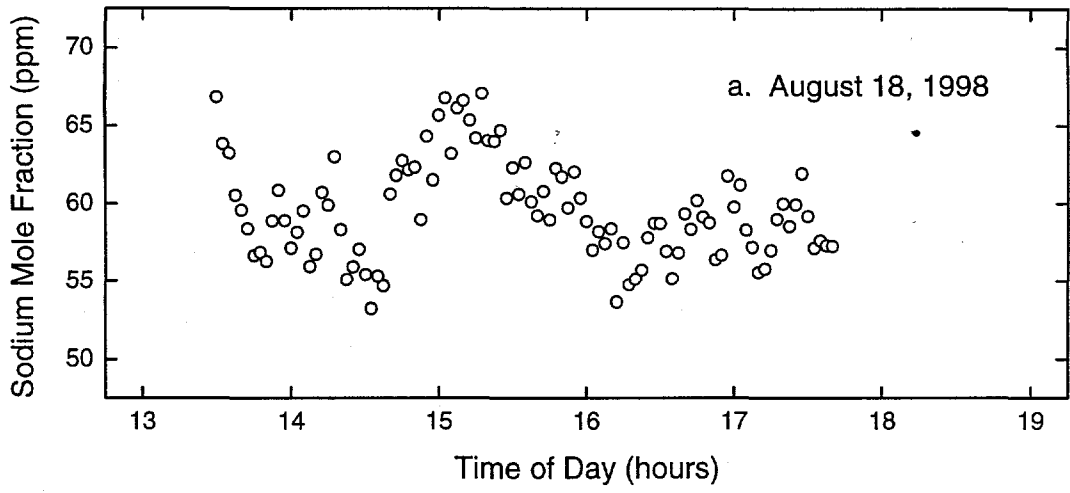


Fig. 5

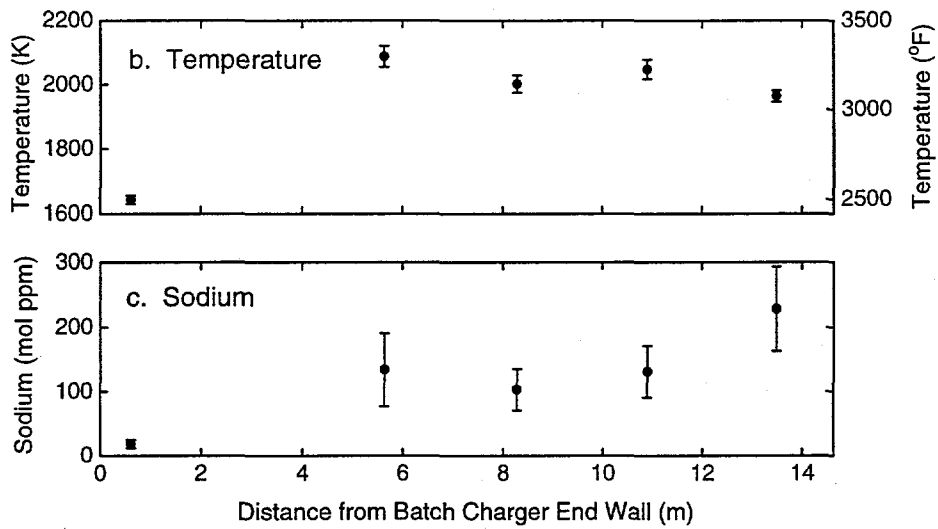
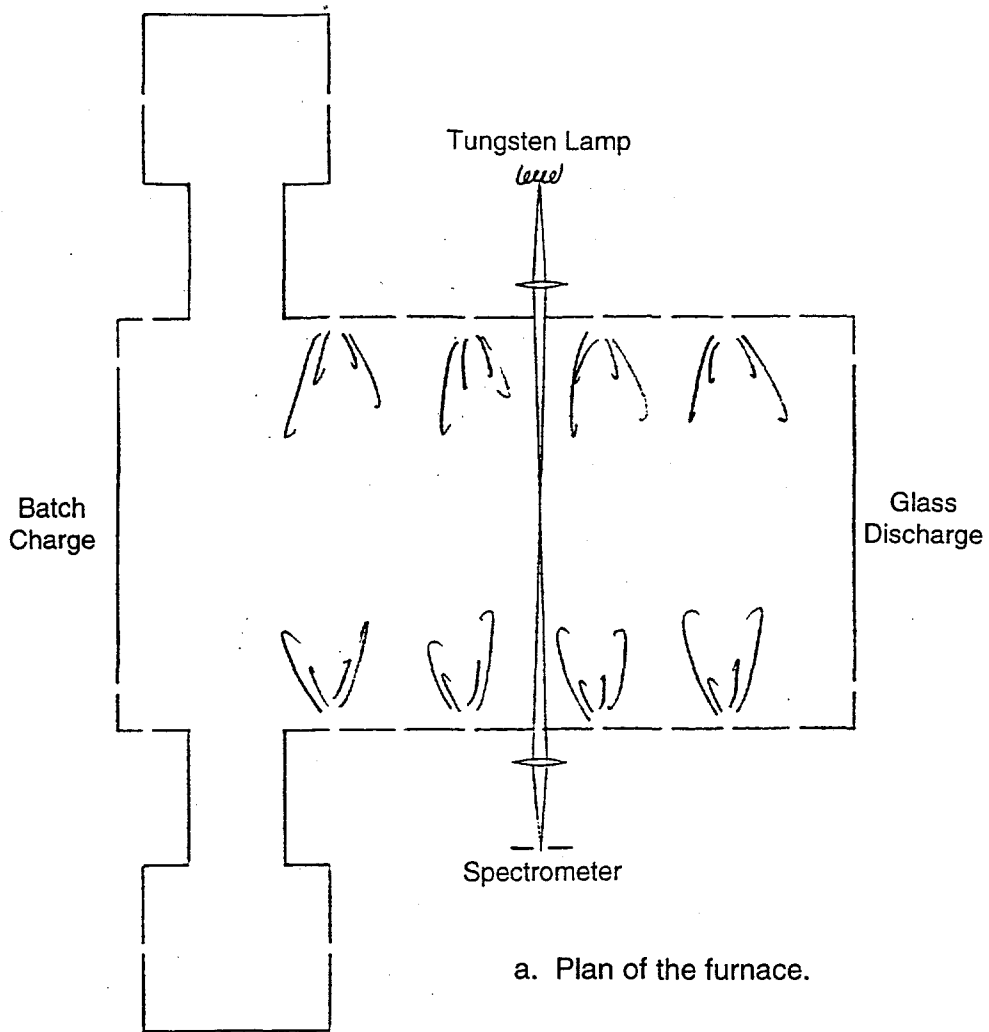


Fig. 6

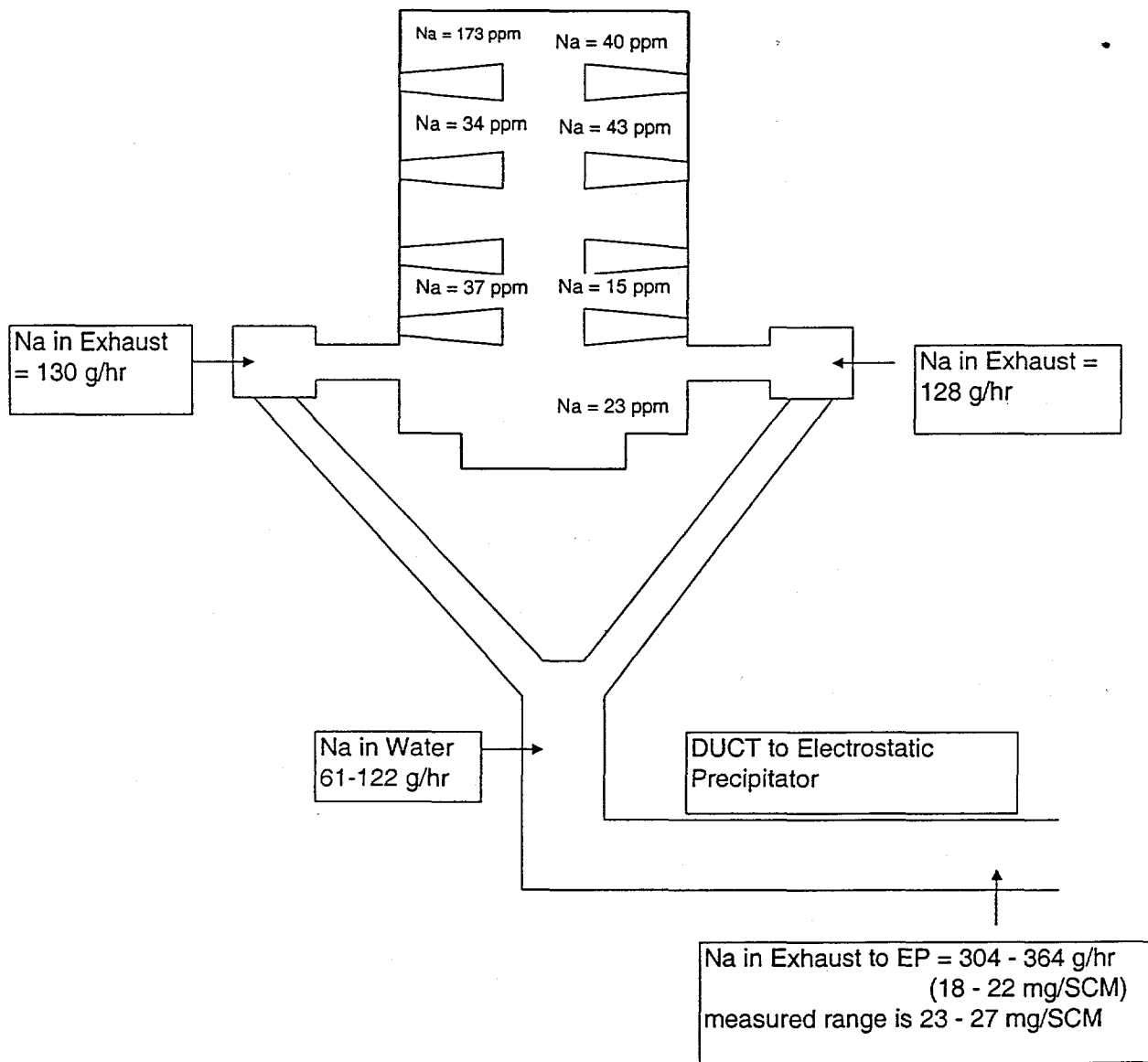


Fig. 7